Stability and Bifurcation Analysis in Transformer Coupled Oscillators

J. Kengne [1]
1- Doctorate School of Electronics (UDETIME)
University of Dchang
Dcshang, Cameroon
kengnemozart@yahoo.fr

J. C. Chedjou [1 2], K. Kyamakya [2], and I. Moussa [1]
2- Institute for Smart- Systems Technologies
University of Klagenfurt
Klagenfurt, Austria
jean.chedjou@uni-klu.ac.at
kyandoghere.kyamakya@uni-klu.ac.at

Abstract— **We derive a simplified mathematical model to describe the nonlinear dynamics of a system consisting of a chaotic transformer-coupled oscillator. This well-known chaotic oscillator is currently modelled by very complex equations which are intractable analytically and numerically as well due to stiffness. The model derived is simple, flexible, accurate and efficient to provide full insight of the dynamics of the oscillator while compared with the well-known classical models. The electronic structure of the oscillator is proposed and sets of nonlinear ordinary differential equations are derived to describe the dynamics of the oscillator. Using the Routh-Hurwitz theorem, the stability analysis of critical points is carried out and conditions for the occurrence of Hopf bifurcations are derived. Various bifurcation scenarios are obtained numerically showing several striking routes to chaos. The biasing current is considered as bifurcation control parameter to highlight the effect of the bias (i.e. power supply) on the dynamics of the oscillator. This is a relevant contribution which enriches the literature as the effect of the bias on the dynamics of such oscillator has not been considered so far by the relevant state-of-the-art. The real physical implementation (i.e. use of electronic components) of the oscillator is considered to validate the simplified model proposed through several comparisons between experimental and numerical results. The bifurcation analysis reveals the possibility for the oscillator to move from near sinusoidal regime to chaos via the usual path of period doubling and sudden transition when monitoring the bias in very tiny windows. Regions of multi-stability are depicted in which coexist various types of attractors.**

Keywords— ***Transformer-coupled oscillators, stability, bifurcation, chaos, coexisting attractors.***

I. INTRODUCTION

The relevant state-of-the-art provides insight/information related to the dynamical behaviour of several chaotic electronic circuits [1-21]. Concerning the modelling, design and realisation of chaotic electronic generators, the following most commonly used approaches can be listed:

a) Designing a universal analogue computing platform to investigate chaos in several types of models (e.g. Lorenz, Chua, and Rössler equations) [2].
b) Tuning classical electronic circuits (e.g. Hartley, Colpitts, and Clapp) in their stiffness mode in order to increase their chaotic potentialities [3]
c) Performing a suitable reconfiguration (e.g. slight modification) of some conventional circuit oscillators and deriving models to explain their complex nonlinear and chaotic dynamics [4-8].
d) Introducing additional nonlinearities (in some conventional structures of nonlinear circuit oscillators) through analogue devices (e.g. transistor, diodes, and Zener diodes): Stability and bifurcation analysis [9-10].
e) Investigating chaos due to nonlinear coupling in conventional circuit oscillators [11].
f) Designing triggered pulse generators to produce/generate broadband chaotic waves [12].

Following the approach mentioned in c), a transformer coupled oscillator is designed and investigated [7]. Using a piece-wise linear (PWL) model for describing the bipolar junction transistor, a PWL model is proposed to investigate the nonlinear phenomenon in transformer-coupled oscillators [7]. However the proposed model in which three nonlinear terms appear is very complex and therefore cannot be easy or flexible to use for investigating the striking and complex bifurcation structures exhibited by this specific type of oscillators. Our aim in this paper is to exploit the same concept to derive a relatively simple model of a transformer coupled oscillator. The proposed model is advantageous as it appears very flexible when dealing with the bifurcation analysis, chaos control and synchronization issues.

The focus on this particular type of oscillator (i.e. the transformer coupled oscillator) can be justified by some good features and characteristics of the oscillator and also the multiple potential applications of the oscillator in engineering. Indeed, the transformer coupled oscillator which is designed using a single bipolar junction transistor is widely used in the fields of electronics and communications. This oscillator is a wideband sinusoidal and/or chaotic waves generator as it can perform from low frequencies (i.e. few Hertz) to high frequencies or microwave frequencies (i.e. few giga-Hertz). Further, this oscillator possesses an intrinsic nonlinearity given by the exponential characteristic of the active device. This characteristic is responsible of the non-symmetric and therefore generic nature of the oscillator. This oscillator which appears to be a standard circuit for setting up harmonic

oscillations can also exhibit rich and complex dynamical scenarios similar to those generated by classical Jerk oscillators (i.e. oscillators modelled by third order ordinary differential equations).

The aim of this paper can be summarised in three key steps. The first is to contribute to the general understanding of the striking dynamical behaviour exhibited by the transformer coupled-oscillator and complete the results obtained so far by deriving a simplified model from which a systematic and methodological analysis of the nonlinear dynamics of the oscillator is carried out. The second is to provide both theoretical and experimental tools, which might serve for design and control purpose. The third is to point out some unknown and striking behaviour of transformer coupled oscillators.

The paper is organised as follows. Section 2 deals with the modelling process. The electronic structure of the oscillator is addressed and the appropriate model (sets of nonlinear ordinary differential equations) is derived to describe the dynamical behaviour of the oscillator. For the sake of simplicity we use an equivalent electronic circuit based on the simpler structure of the bipolar junction transistor. Section 3 is concerned with the analysis of the stability of equilibrium points (in the linear response) and the investigation of the local bifurcations exhibited by the transformer-coupled oscillator. Section 4 considers the numerical study. The effect of the bias on the dynamical behaviour of the oscillator is examined. Various phase portraits and bifurcation diagrams associated with their corresponding graphs of largest numerical 1-D Lyapunov exponents are obtained to define the nature of transitions/routes to chaos. Section-5 deals with the experimental study. The real physical implementation of the oscillator is carried out using electronic circuits. Experimental results are compared with numerical results and a very good agreement is observed which serves to validate the model derived in this paper. Section 6 deals with concluding remarks and proposals for future works.

II. CIRCUIT DESCRIPTION AND STATE EQUATIONS

A. Circuit Description

The schematic diagram of the transformer coupled oscillator under investigation is depicted in Fig.1. The bipolar junction transistor Q_1 used in the common-base configuration, plays the role of nonlinear gain element. A positive feedback is provided by the transformer and the capacitor C_2. The coupling capacitor C_0 which is being used to prevent DC bias current from flowing through the tank circuit might have very low impedance at operating frequencies. The parallel resonant circuit consists of the resistor R, the capacitor C_1 and the transformer L_1 / L_2. I_{EE} is an ideal current source used to adjust the DC bias. The fundamental frequency of the transformer coupled oscillator can be estimated [7] as follows:

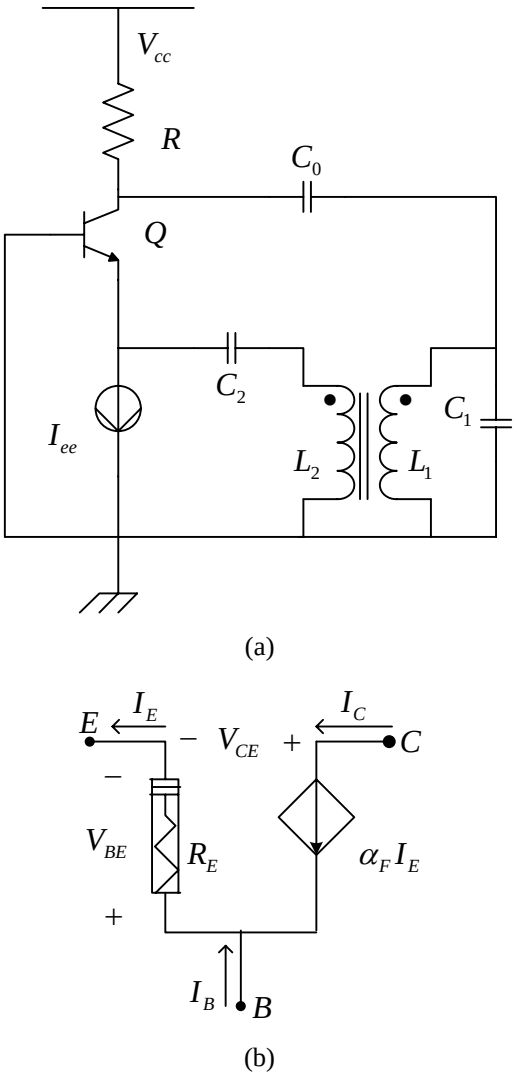

Fig.1: Circuit diagram of the transformer coupled oscillator (a) and the BJT model consisting of one current controlled current source and a single diode (b).

$$f_0 = \frac{1}{2\pi}\sqrt{\frac{1}{LC_1} + \frac{1+\beta}{Rr_\pi C_1 C_2}} \tag{1}$$

where β and r_π are the parameters of the bipolar junction transistor (BJT) Q_1 at the operating point. The transistor Q_1 which represents the source of nonlinearity in the oscillator is responsible of the striking and chaotic motions exhibited by the oscillator. Note that the resistor R is used both for damping purpose and biasing. Conversely to the series-fed structure proposed in ref. [7] no base resistor is needed. Further, the resonant network is shunt-fed. These are essential/key modifications we are proposing which aim at deriving a simplified mathematical model of the oscillator. The model derived is simplified in terms of the number of parameters involved and the number of nonlinear terms. In both cases the number of parameters is less when compared to the well-

known model of the same oscillator proposed by the relevant literature.

As previously discussed in ref. [7], we emphasize that the transformer coupled oscillator depicted in Fig.1 exhibits a certain degree of universality, since other components, such as capacitor or inductor dividers can often be replaced by an equivalent transformer-coupled structure. Thus, a transformer coupled oscillator represents a standard circuit for setting up harmonic oscillations.

B. State Equation

According to the standard approach followed in the qualitative analysis [13] of nonlinear systems, we select a minimal model for the transformer coupled oscillator, i.e as simple as possible which maintains the essential features exhibited by the real oscillator. Henceforth, we assume that both passive and reactive elements are ideal. Further four main/key assumptions are envisaged to ease the modelling process. The first assumption considers that the transistor Q_1 is modelled by a nonlinear resistor R_E and a linear current-controlled current source [4], as shown in Fig.1 (b). The second assumption models the base-emitter (B-E) driving point characteristic with an exponential function, namely:

$$I_E = f\left(V_{BE}\right) = I_S\left[\exp\left(\frac{V_{BE}}{V_T}\right)-1\right] \tag{2}$$

where I_E is the emitter current, V_{BE} is the voltage across the B-E junction, I_S is the saturation current of the B-E junction, α_F is the common base forward short-circuit current gain of the transistor, and $V_T = k_b T / q$ is the thermal voltage. k_b is the Boltzmann constant, T is the absolute temperature expressed in Kevin, and q is the electron charge. Note that $V_T \approx 26mV$ at room temperature (i.e. 300K). The third assumption neglects the parasitic effects in capacitors C_{be} and C_{ce} at operating frequencies. The fourth assumption supposes the transformer $\left(L_1 / L_2\right)$ to be operating within its linear region.

If we denote by I_L the current flowing through the inductor L, and $V_{C_i}\left(i=0,1,2\right)$ the voltage across capacitor $C_i\left(i=0,1,2\right)$; the Kirchhoff current law (KCL) and the Kirchhoff voltage law (KVL) can be applied to the circuit in Fig.1 to obtain the following set of autonomous ordinary differential equations describing the dynamics of the system (V_{C_0} is assumed constant due to the relatively large value of the coupling capacitance C_0) :

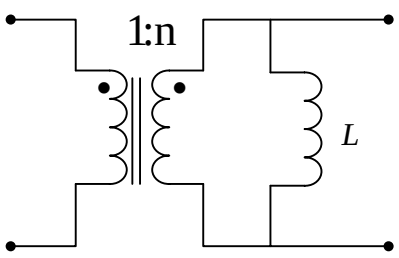

Fig. 2: Transformer model used for modelling. L is the magnetizing inductance of the transformer ($L = L_1 + n^2 L_2$).

$$C_1 \frac{dV_{C_1}}{dt} = -\frac{V_{C_1}}{R} + \frac{V_{cc} - V_{C_0}}{R} - I_L + \left(-\alpha_F + \frac{1}{n}\right) I_E - \frac{I_{ee}}{n} \tag{3a}$$

$$C_2 \frac{dV_{C_2}}{dt} = I_E - I_{ee} \tag{3b}$$

$$L \frac{dI_L}{dt} = V_{C_1} \tag{3c}$$

where

$$I_E = f\left(V_{BE}\right) = I_S\left(\exp\left(V_{BE}/V_T\right)-1\right) \tag{3d}$$

and $V_{BE} = -V_{C_2} - V_{C_1}/n$ is the base-emitter voltage.

It can be shown from Eqs. (3) the existence of a single equilibrium point located in the so called forward active region (referring to the PWL model of the oscillator). This equilibrium point $\left(\overline{V_{C_1}}, \overline{V_{C_2}}, \overline{I_L}\right)^T$ is obtained by setting the right hand side of Eqs. (3) to zero; thus:

$$\left(\overline{V_{C_1}},\ \overline{V_{C_2}},\ \overline{I_L}\right)^T = \left(0,\ V_T \ln\left(I_S / I_{ee}\right),\ 0\right)^T \tag{4}$$

A suitable change of variables and parameters is performed ($x_i V_T = V_{C_i} - \overline{V_{C_i}}\left(i=1,2\right)$, $x_3 V_T = \rho\left(I_L - \overline{I_L}\right)$, $t = \tau\sqrt{LC_1}$, $\rho = \sqrt{L/C_1}$, $\in = C_1/C_2$, $\alpha = \rho/R$, and $\gamma = \rho I_{ee}/V_T$) to transform Eqs. (3) into the following sets of normalized nonlinear ordinary differential equations:

$$\frac{dx_1}{d\tau} = -\alpha x_1 - x_3 + \gamma\left(-\alpha_F + 1/n\right)\phi\left(x_1, x_2\right) \tag{5a}$$

$$\frac{dx_2}{d\tau} = \in \gamma\phi\left(x_1, x_2\right) \tag{5b}$$

$$\frac{dx_3}{d\tau} = x_1 \tag{5c}$$

where

$$\phi\left(x_1, x_2\right) = \exp\left(-x_2 - x_1/n\right) - 1 \tag{5d}$$

It should be worth noticing the relative simplicity of our model in Eqs. (5). The nonlinearity appears twice and only two state variables are involved. This simplicity of the state equations might allow an in-depth analysis of the dynamics of the transformer-coupled oscillators. Further, with such a simplified model, investigations based on chaos control and synchronization of these types of oscillators might be performed in a systematic manner. It is also necessary to mention that i_L is the current flowing through the magnetising inductor of the transformer network and consequently cannot be measured in real experiment.

III. STABILITY ANALYSIS

An important step towards the stability analysis could be evaluating the volume contraction of the oscillator modelled by Eqs. (5) in order to get preliminary insights of the types of attractors (stable or unstable) which might coexist in the system.

We recall that the volume contraction rate of a dynamical system described by $\frac{dX}{dt} = F\left(X\right)$, where $X = \left(x, y, z\right)^T$ and $F\left(X\right) = \left(f_1\left(X\right), f_2\left(X\right), f_3\left(X\right)\right)^T$ is given by Eq. (6a).

$$\Lambda = \nabla.F\left(X\right) = \frac{\partial f_1}{\partial x} + \frac{\partial f_2}{\partial y} + \frac{\partial f_3}{\partial z} \tag{6a}$$

If Λ is constant, then the time evolution in phase space is determined by $V\left(t\right) = V_0 e^{\Lambda t}$ where $V_0 = V\left(t = 0\right)$. Therefore, a negative value of Λ leads to a fast exponential shrinks (i.e. damped) of the volume in phase space; the dynamical system is dissipative and can exhibit or present stable attractors. For $\Lambda = 0$, the phase space volume is conserved and the dynamical system is conservative. If Λ is positive, the volume in phase space expands and hence there exist only unstable fixed points or cycles or possibly chaotic repellors i.e., the dynamics diverges at long term (i.e. $t \to \infty$) if the initial conditions do not lie exactly on one of the fixed points or stationary states.

Referring to the model in Eqs. (5) it can be shown that $\Lambda = \nabla.F\left(X\right)$ reads:

$$\Lambda = -\alpha - \gamma\left(\left(-\alpha_F + \frac{1}{n}\right)\frac{1}{n} + \in\right)\exp\left(-x_2 - x_1/n\right) \tag{6b}$$

Then, if we select α_F such that $\alpha_F < n \in +1/n$, then $\Lambda \le 0$ for all x_i, and consequently our model would be dissipative thus the system can support stable attractors; otherwise the model in Eqs. (5) can exhibit only unstable attractors.

´The stability analysis is carried out by transforming Eqs. (5) into the following form:

$$\frac{dV}{dt} = F\left(V, \mu\right)$$

where $V = \left(x_1, x_2, x_3\right)$ is an autonomous vector field and $\mu = \left(\varepsilon, \alpha, \gamma, n, \alpha_F\right)$ an element of the parameter space. Eqs. (5) generate a flow $\phi = \left\{\phi^T\right\}$ on the phase space $R^3 \times S^1$ and there exist a global map:

$$P : \sum_C \to \sum_C$$

$$V_p\left(x_1, x_2, x_3\right) \to P\left(V_p\right) = \left\{\phi^T\right\}\Big|_{\sum_C\left(x_1, x_2, x_3\right)}$$

where $\left(x_1, x_2, x_3\right)$ represents the coordinates of the projection of the attractors onto the Poincaré cross section $\sum_C$ defined by $\sum_C = \left\{\left(x_1, x_2, x_3\right) \in R^3 \times S^1\right\}$. The perturbation analysis [14-15] is used to investigate the stability of solutions in the Poincaré map $\sum_C$. Thus, Eqs. (5) can be perturbed by adding a small perturbation $\delta V_P\left(\delta x_1, \delta x_2, \delta x_3\right)$ to the steady state $V_{PO}\left(x_{10}, x_{20}, x_{30}\right)$. The following variational differential equation

$$\frac{d\delta V_P}{dt} = DF\left(V_{PO}\right)\delta V_P$$

where

$$DF\left(V_{PO}\right) = \begin{bmatrix} -\alpha - \frac{\in_2}{n}\psi_0 & -\in_2 \psi_0 & -1 \\ -\frac{\in_1}{n}\psi_0 & -\in_1 \psi_0 & 0 \\ 1 & 0 & 0 \end{bmatrix} \tag{7}$$

is obtained by developing coefficients of the perturbed Eq.(5) into powers of the small perturbations $\left(\in_1=\in\gamma, \in_2=\gamma\left(-\alpha_F+1/n\right), \psi_0=\exp\left(-x_{20}-x_{10}/n\right)\right)$. $DF\left(V_{PO}\right)$ is a 3×3 Jacobian matrix describing the vector field along the solution $\delta V_P\left(t\right)$. Our analysis is restricted to the case of small amplitudes of the steady state. The stability of the periodic motion is obtained according to the real parts of the roots of the following characteristic equation $\left(\det\left[DF\left(V_{PO}\right)-\lambda I_d\right]=0\right)$

$$\lambda^3+\left(\alpha+\in_1+\frac{\in_2}{n}\right)\lambda^2+\left(1+\alpha\in_1\right)\lambda+\in_1=0 \qquad (8)$$

obtained by considering small amplitudes of the steady states. Fig. 3 shows (in the complex plane $\left(\mathrm{Re}\left(\lambda\right),\mathrm{Im}\left(\lambda\right)\right)$) the representation of the eigenvalues (roots of the characteristic equation). These roots are obtained (using the Newton-Raphson algorithm) for $\in=1/12$ with $\alpha\in\left[0.51,3.69\right]$ and $\gamma\in\left[4.96,39.72\right]$. From Fig. 3 one can have an idea on both the stability of periodic solutions and the different types of bifurcation likely to appear in the system. $DF\left(V_{PO}\right)$ being a real matrix, complex eigenvalues in complex conjugate pairs are responsible of the observed symmetry along the real axis. Thus if the real parts of the eigenvalues $\left(\lambda\right)$ are all negative, the rate is of the contraction type or otherwise of the expansion. If the eigenvalues are all real, the contraction or the expansion is observed near the steady state while the complex values of the eigenvalues show the contraction or expansion of the spiral. If there exist eigenvalues having real parts with different sign, the equilibrium state is called saddle; an equilibrium point whose eigenvalues have nonzero real parts is called hyperbolic. On the other hand period doubling bifurcation is observed if there exists an eigenvalue $\left(\lambda=-1\right)$ while bifurcations of the Hopf type are observed if the following conditions are satisfied: a) there exists a pair of pure imaginary complex conjugate eigenvalues; b) $d\lambda/d\alpha\big|_{\alpha=\alpha_c}\neq0$, α being the bifurcation control parameter. α_c is the critical value for the occurrence of Hopf bifurcation, obtained from the equation $\mathrm{Re}\left(\lambda\right)=0$. It can be derived using the Routh-Hurwitz criterion that the equilibrium point $O\left(0\ ,\ 0\ ,\ 0\right)^T$ is stable if and only if the following analytic relations are satisfied:

$$\alpha+\in_1+\frac{\in_2}{n}>0 \qquad (9a)$$

$$\alpha+\frac{\in_2}{n}+\alpha\in_1^2+\alpha^2\in_1+\alpha\frac{\in_1\in_2}{n}>0 \qquad (9b)$$

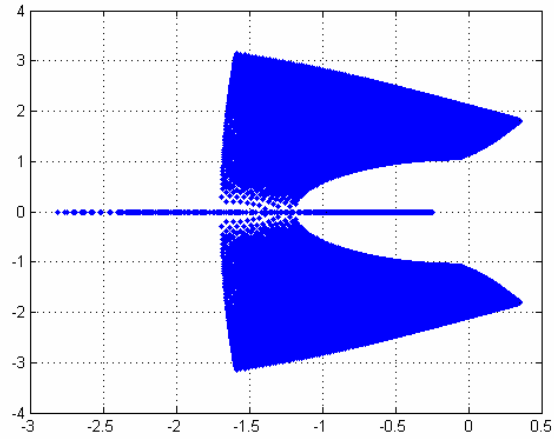

Fig.3: Representation of the eigenvalues solutions in the complex plane ($\mathrm{Re}\left(\lambda\right)$ $\mathrm{Im}\left(\lambda\right)$).

Using the coefficient α as control parameter, we have derived the following critical relationships between the parameters of the model in Eqs. (5) (describing the dynamics of the transformer coupled oscillator) for the occurrence of the Hopf bifurcation of fixed point $O\left(0\ ,\ 0\ ,\ 0\right)^T$:

$$\omega_H^2=1+\alpha_c\in_1 \qquad (10a)$$

$$\in_1\alpha_c^2+\left(1+\in_1^2+\frac{\in_1\in_2}{n}\right)\alpha_c+\frac{\in_2}{n}=0 \qquad (10b)$$

$$1+2\in_1\alpha_c+\in_1^2+\frac{\in_1\in_2}{n}\neq0 \qquad (10c)$$

Eq. (10b) has two roots with opposite sign for $\in_2\leq0$ (i.e. for $-\alpha_F+1/n\geq0$); thus if $\left(-\alpha_F+1/n\leq0\right)$ no Hopf bifurcation is possible. For $\in_2\leq0$, the critical value of α_c is expressed as follows:

$$\alpha_c=\frac{-\left(1+\in_1^2+\in_1\in_2/n\right)+\sqrt{\Delta}}{2\in_1} \qquad (11a)$$

where

$$\Delta=\left(1+\in_1^2+\in_1\in_2/n\right)^2-4\in_1\in_2/n \qquad (11b)$$

Substituting $\lambda_{1,2}=\pm j\omega_H$ into Eq. (8) we obtain the third root $\lambda_R=-\alpha_c-\in_1-\in_2/n$ which is the real eigenvalue, the other two roots being $\lambda_{1,2}$. Considering the previous

results it clearly appears (see Fig. 3) that our system of the given parameters α and γ can undergo various types of bifurcations, namely, saddle, period-doubling and Hopf bifurcation. Note that the universal Chua circuit is currently used to demonstrate the existence of various types of bifurcation scenarios [2] amongst which can be found the bifurcation scenarios discussed in this work.

IV. NUMERICAL STUDY

The aim of the numerical study is to display the system's attractors related to various types of behaviour and to define scenarios leading to chaos. This is achieved through a direct integration of the state equations (Eqs. (5)). Further, due to the fact that chaos is characterized by its complexity, unpredictability, and extreme sensibility to initial conditions, the investigation of the effects of initial conditions on the behaviour of the oscillator is also considered.

A. Chaotic behavior

Eqs. (5) are solved numerically to define routes to chaos using the fourth-order Runge-Kutta algorithm. For the set of parameters used in this work, the time step is always $\Delta t \le 0.005$ and computations are performed using variables and constants parameters in extended mode. The integration time is always $T \ge 10^6$. Three indicators are used to identify the type of motion. The first indicator is the bifurcation diagram; the second is the FFT spectrum and the third is the largest one dimensional (1D) numerical Lyapunov exponent defined by:

$$\lambda_{\max} = \lim_{t\to\infty}\left[(1/t)\ln\left(d\left(t\right)\right)\right] \qquad (12a)$$

where

$$d\left(t\right) = \sqrt{\xi_1^2 + \xi_2^2 + \xi_3^2} \qquad (12b)$$

and computed from the following variational equations

$$\dot{\xi}_1 = -\alpha\xi_1 - \in_2 \left(-\xi_2 - \xi_1/n\right)\exp\left(-x_2 - x_1/n\right) \qquad (13a)$$

$$\dot{\xi}_2 = \in_1 \left(-\xi_2 - \xi_1/n\right)\exp\left(-x_2 - x_1/n\right) \qquad (13b)$$

$$\dot{\xi}_3 = \xi_1 \qquad (13c)$$

obtained by perturbing the solutions of Eqs. (5) as follows: $x_1 \to x_1 + \xi_1$, $x_2 \to x_2 + \xi_2$, $x_3 \to x_3 + \xi_3$. $d\left(t\right)$ is the distance between neighbouring trajectories. Asymptotically $d\left(t\right) = \exp\left(\lambda_{\max} t\right)$. Thus, if $\lambda_{\max} > 0$, neighbouring trajectories diverge and the state of the oscillator is chaotic. For $\lambda_{\max} < 0$, these trajectories converge and the state of the oscillator is non-chaotic. The case $\lambda_{\max} = 0$ corresponds to the torus state of the oscillator.

In order to analyse the effects of biasing on the dynamics of the oscillator, I_{ee} is chosen as control parameter and the circuit components in Fig.1 are defined as follows: $R = 500\Omega$, $C_1 = 6nF$, $C_2 = 72nF$, $C_3 = 22uF$, $L = 400\mu H$, $n = 10$ $V_{cc} = 12V$, $\alpha_F = 250$. Therefore a scanning process is performed to investigate the sensitivity of the oscillator to tiny changes in I_{ee}. The range $0 \le I_{ee} \le 4mA$ is considered to monitor the bifurcation control parameter. The scanning process has revealed that the oscillator in Fig.1 can exhibit complex dynamical states namely, multi-periodic, quasi-periodic, and chaotic states. Similar results were observed and depicted in Refs. [16-17]. Indeed, for the values of electronic components defined above, various routes to chaos are observed such as period doubling, sudden transitions, and period adding scenarios to chaos. Fig. 4 shows a bifurcation diagram associated with the corresponding graph of largest 1D largest numerical Lyapunov exponent. This bifurcation diagram shows the state of the voltage v_1 across the capacitor C_1 (attractor) in terms of the biasing current I_{ee} (control parameter). As it appears in Fig. 4, two different routes to chaos are obtained in terms of

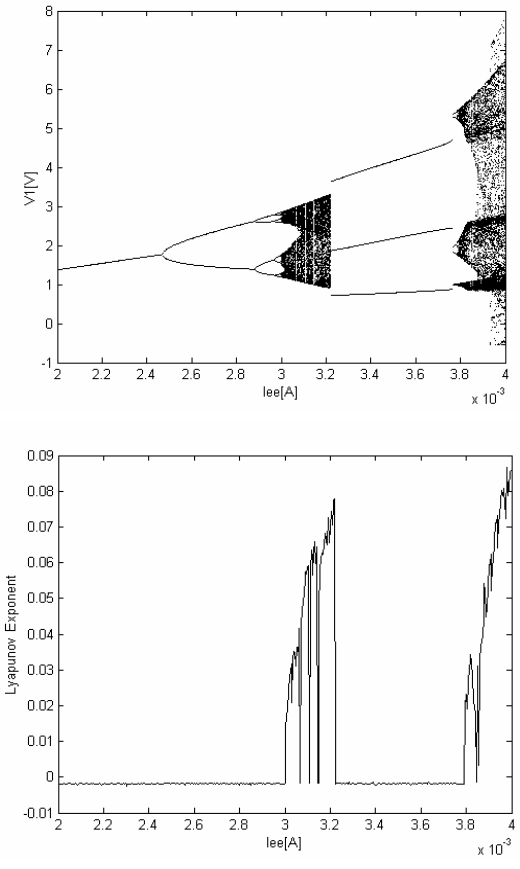

Fig. 4: Bifurcation diagram of the oscillator and the corresponding graph of 1D largest num. Lyapunov exponent in terms of the control parameter I_{ee}.

the control parameter. The first route to chaos is achieved through period doubling scenario while the second route to chaos is through a period-3 sudden transition scenario. Further, windows of chaotic states of the oscillator alternating with those of regular motion are obtained. The weak chaoticity (degree of chaos) of the oscillator is clearly justified by the small values of the largest 1D numerical Lyapunov exponent that are always less than 0.09.

Using the same values of parameters in Fig. 4 various numerical computations of the phase portraits of the oscillator associated with their corresponding FFT spectra (see a sample result in Fig. 5) were obtained confirming transitions/routes to chaos depicted previously. Indeed we have obtained the complete scenarios to chaos presented in Fig. 4. Specifically,

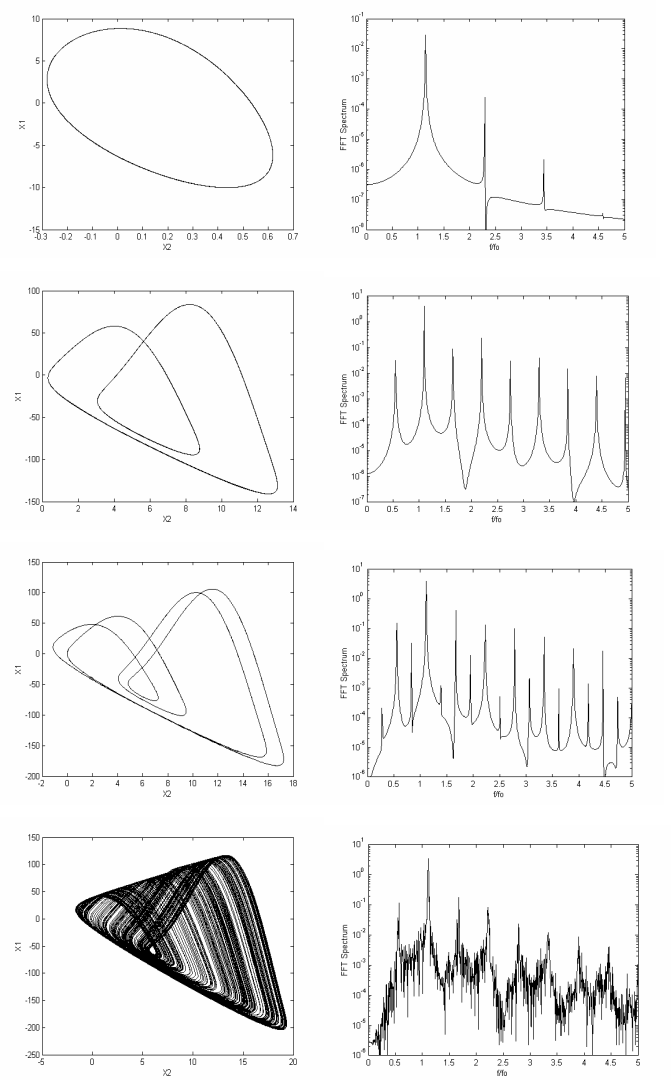

Fig.5: Numerical phase portraits of the voltage across capacitor *C1* (left) and the corresponding FFT spectra (right) obtained for the following values: (a) $I_{ee} = 0.8mA$, (b) $I_{ee} = 2.6mA$, (c) $I_{ee} = 2.95mA$, (d) $I_{ee} = 3.10mA$.

the following scenario was observed when monitoring the control parameter: period 1 $\rightarrow$ period 2 $\rightarrow$ period 4 $\rightarrow$ period 8 $\rightarrow$ chaos $\rightarrow$ period 3 $\rightarrow$ chaos. Fig. 5 shows a sample result of the period doubling scenario to chaos we observed by plotting phases portraits with their corresponding FFT. Concerning the FFT process, the periodicity of the attractor (i.e. the total number of frequencies in a wave) is deduced by neglecting/ignoring frequency spectrums with small amplitudes.

An interesting analogy was observed when comparing the circuit oscillator we have considered in this work (see Fig.1) with the one previously discussed in ref. [7]. Indeed, it should be noted that both circuits (shunt-fed and series-fed structures) posses the same family of attractors. Further, the position of the tank network doesn't influence the nature of the attractor. The various transitions/routes to chaos observed in the transformer-coupled oscillator are commonly observed in nonlinear systems [2], such as forced systems, coupled autonomous systems, and coupled forced systems [15], just to name a few. Although the biasing current (i.e. the parameter γ) has been used as control parameter in this work, it should be worth noticing that any other component (or parameter) that appears in the characteristic equation can serve as a bifurcation control parameter.

B. Coexistence of attractors

An interesting phenomenon we observed during our numerical computations is the extreme sensitivity of the dynamics of the oscillator to initial conditions. This sensitivity is illustrated in Fig. 6 where for well-specified values of the system parameters (i.e. $\gamma = 317.78$, $\in$=1/12 , α=0.5164) two different attractors are obtained by changing the initial conditions. Indeed, the chaotic attractor in Fig. 6a corresponds to the initial conditions $x_{10} = 0$, $x_{20} = 20$, $x_{30} = 0.05$ while the initial conditions $x_{10} = 20$, $x_{20} = 20$, $x_{30} = 0.05$ lead to the regular attractor in Fig 6b. This interesting result confirms a possible coexistence of attractors (regular and/or chaotic) in dissipative nonlinear systems. Such systems are good prototypes to exhibit multiple dynamic equilibrium states for the same set of system parameters. Note that the coexistence of multiple attractors is an exciting phenomenon in nonlinear dynamics as it leads to various technological applications [18]. Such a phenomenon, referred to as generalized multi-stability, has been observed in various systems including electronic circuits, lasers, and mechanical and biological systems [18]. Finally mention that such a phenomenon has also been reported by Maggio et al. [6] when investigating the nonlinear behaviour of the Colpitts oscillator.

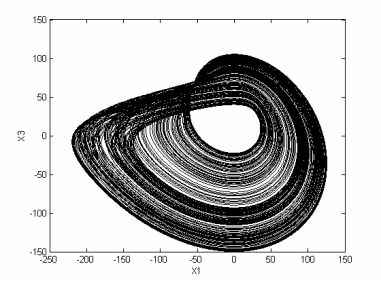

(a)

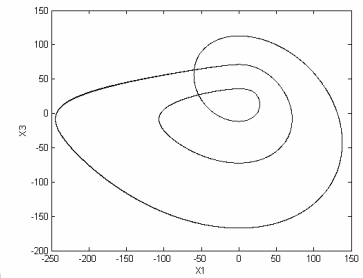

(b)

Fig. 6: Projections of the attractors on the (x_1, x_3) plane showing the coexistence of a chaotic attractor and a period-3 limit cycle when the system parameters are set to the following values: $\gamma = 317.78$, $\in$ =1/12 , α=0.5164

V. EXPERIMENTAL STUDY

A. *Design and real physical implementation*

According to previous results, the transformer coupled oscillator can experience complex and striking bifurcation scenarios leading to chaos when monitoring the biasing current I_{ee}. Our aim in this part is to verify these results experimentally. The experimental set up in Fig. 7 is a proposal of the design and implementation (on electronic breadboard) of the transformer coupled oscillator shown in Fig. 1. The following values of circuit components are used: $R = 500\Omega$, $C_1 = 6nF$, $C_2 = 72nF$, $L = 400\mu H$, $n = 10$, and $V_{cc} = 12V$. To insure or guaranty good functioning of the circuit implemented on breadboard the power transmission must be well controlled at critical points of the complete circuit in Fig. 7. Thus, the network consisting of the operational amplifier U_1 is envisaged to implement an ideal current generator if the following condition is fulfilled:

$$\frac{R_1}{R_2} = \frac{R_3}{R_4 + R_5} \qquad (14a)$$

The current I_{ee} pulled from the load is given by:

$$I_{ee} = \frac{R_2}{R_1 R_5} V_i \qquad (14b)$$

where V_i is the output voltage of the network (i.e. an inverting amplifier) using the operational amplifier U_2. Eqs. (14a) and (14b) can be exploited together with the values of the circuit components in Fig. 7 to derive the following relationship between the control voltage V_i and the current I_{ee}:

$$I_{ee} = \frac{V_i}{1000} \qquad (14c)$$

Thus, I_{ee} is supposed to vary between 0 and 12mA as R_{10} varies between 0 and $100\,k\Omega$ since the input of the amplifier U_2 is connected to -12V.

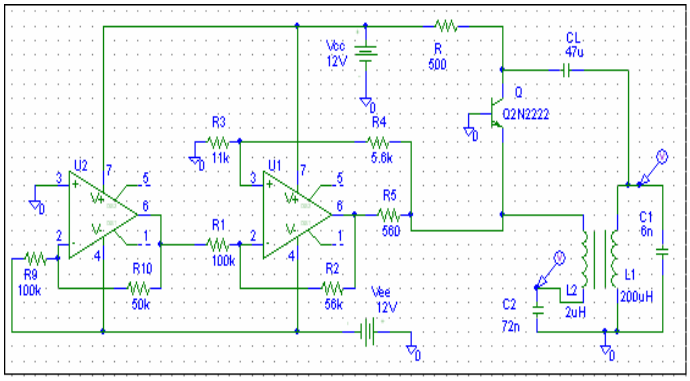

Fig.7: Experimental setup for measurement on the transformer coupled oscillator

B. *Experimental results*

We now want to investigate the effects of the biasing current I_{ee} (i.e. control parameter) on the dynamics of the circuit oscillator. The control resistor is R_{10} which insures the variation of I_{ee}. The experimental results are obtained showing phase portraits which are plots in the phase-space materialized by the voltage across capacitor C_1 (V_{C_1}) in terms of the voltage across capacitor C_2 (V_{C_2}). The experimental results have revealed that the dynamics of the oscillator changes substantially as I_{ee} is monitored. This is clearly demonstrated by the experimental pictures in Fig. 8 showing the real behaviour of the transformer coupled oscillator under investigation. As it appears in Fig. 8, the real circuit shows the same bifurcation scenarios as observed using numerical method. Indeed the experimental phase portraits in Fig. 8 reveal/show an evolution of the system starting from near-sinusoidal oscillations to chaos via a period doubling sequence when I_{ee} is increased. This evolution shows similar experimental bifurcation scenarios (period-1 $\rightarrow$ period-2 $\rightarrow$ period-4 $\rightarrow$ period-8 $\rightarrow$ chaos) as depicted numerically. The experimental results obtained were generally very close both qualitatively and quantitatively to numerical results. The results in Fig. 8 confirm a good agreement between numerical

results and experimental results and thereby can be considered to validate the model derived in this work (Eqs. 5) to describe the dynamical behaviour of the transformer coupled oscillator.

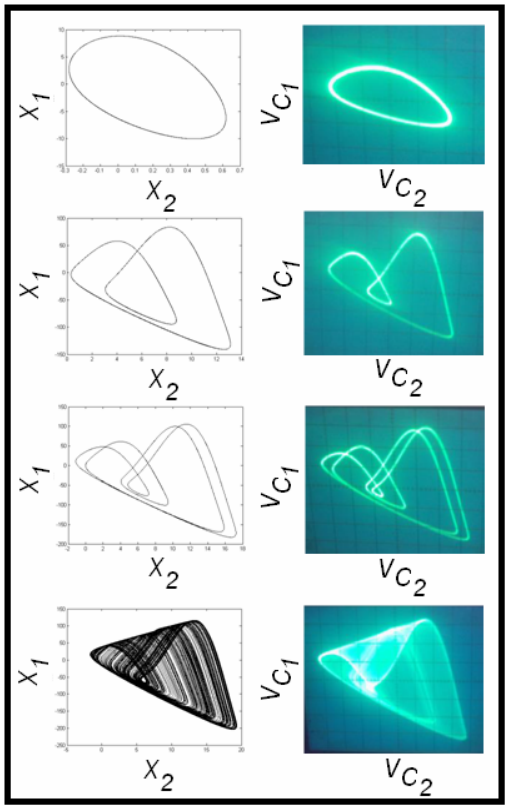

Fig.8: Experimental phase portraits (right) obtained from the circuit (Ch_1: V_{C_2} ; Ch_2 : V_{C_1}): a) period-1 for $I_{ee} = 1.5mA$; b) period-2 for $I_{ee} = 3.2mA$; c) period-4 for $I_{ee} = 3.5mA$; d) chaotic attractor for $I_{ee} = 4mA$. The scales are (X axis: 10mV/div; Y axis:0.5V/div) for (a) and (X axis: 0.1V/div; Y axis: 2V/div) for (b), (c) and (d). The corresponding numerical phase portraits are shown left.

VI. CONCLUSION

In this paper, we have introduced and analysed a simplified structure of a transformer-coupled oscillator. The choice of this type of oscillator was mainly motivated by its multiple potential applications in engineering and in communications. The interest to introducing a simplified model was found in the flexibility of the new structure proposed and the ease manipulation of the parameter settings of this structure to analyse the complex and striking bifurcation exhibited leading to several transitions/routes to chaos. The electronic structure of the oscillator was proposed and the modelling process was performed to derive sets of ordinary differential equations describing the behaviour of the oscillator. The stability of the system was investigated and analytical criteria for the occurrence of Hopf bifurcation were derived. Various bifurcation diagrams associated to their graph of 1D largest numerical Lyapunov exponent were obtained showing period doubling, period adding and abrupt/sudden transition routes to chaos. It was shown that the structure of the transformer-coupled oscillator considered in this work can exhibit near sinusoidal oscillations, sub-harmonics and chaotic oscillations. To highlight the effects of biasing on the dynamics of this particular oscillator, I_{ee} was chosen as control parameter. The extreme sensitivity of the dynamical behaviour of the oscillator to tiny changes in I_{ee} was shown. Also shown was the extreme sensitivity of our model to initial conditions. This sensitivity was explained by the presence of coexisting attractors both in their regular and chaotic regime. Analytical, numerical and experimental results were compared and a very good agreement was observed.

An interesting question under consideration is that of developing synchronization schemes for promoting synchronization based design [21-22] of such oscillators. Such an investigation is of high importance in many applications areas such as chaotic secured communications where chaos synchronization is being exploited in wave coding processes. Another problem under consideration is that of extending the above analysis to the investigation of the nonlinear dynamics in the Hartley oscillator, which is another third order classical oscillator currently used in practice. It would be of interest carrying out a systematic analysis of the effects of initial conditions on the dynamics of the oscillator considered in this work. Such a study can lead to the plot of many basins (chaotic or regular) of attraction which will be of precious use for design engineers of complex nonlinear oscillators.

REFERENCES

[1] L. M. Pecora and T. L. Carroll, Phys. Rev. Lett. 64, 821 (1990).

[2] L. O. Chua, C. W. Wu, A. Huang, and G. Q. Zhong, “A universal circuit for studying and generating chaos-Part I: Routes to chaos”, IEEE Transaction on Circuits and Systems-1, vol.40, No.10, pp.731-744, 1993.

[3] J. C. Liu, H. C. Chou, and J. H. Chou, ”Clarifying the chaotic phenomenon in an oscillator by Lur’e system form”, Microwave and Opt. Tech. Letters, Vol. 22, pp. 323-328, 1999.

[4] M. Kennedy “Chaos in the Colpitts oscillator”. IEEE Transaction on Circuits and Systems-1, vol.41, pp.771-774, 1994.

[5] M. P. Kennedy, “On the relationship between chaotic Colpitts oscillator and Chua’s circuit”,

IEEE Transaction on Circuits and Systems, CAS-42, pp.373-376, 1995.

[6] G. M. Maggio, O. De Feo and M. P. Kennedy, “Nonlinear analysis of the Colpitts oscillator and application to design”, IEEE Transaction on Circuits and Systems, CAS-46, pp.1118-1130, 1999.

[7] J. Zhang, “Investigation of chaos and nonlinear dynamical behaviour in two different self-driven oscillators”, PhD thesis, University of London, 2001.

[8] J. Zhang, X. Chen and A.C. Davies, “Loop Gain and its Association with the nonlinear behaviour and chaos in a Transformer Coupled Oscillator”, International journal of Bifurcation and Chaos, vol.14, N°7, 2004, pp.2503-2512.

[9] A. S. Elwakil, A. M. Soliman, “Two modified for chaos negative impedance converter op amp oscillators with symmetrical and anti-symmetrical nonlinearities”, International Journal of Bifurcation and Chaos, Vol.8, N°6 (1998) 1335-1346.

[10] A. Najumas and A. Tamasevicius. “Modified Wien-bridge oscillator for chaos”. Electronics letter, 31, pp.335-336, 1995.

[11] Y. Hosokawa, Y. Nishio and Akio Ushida, “Analysis of Chaotic Phenomenon in two RC Phase Shift Oscillators Coupled by a diode”, IEICE Trans. Fundamentals, Vol.E84-A, N°9 September 2001.

[12] Nikolai F. Rulkov and Alexander R. Volkovskii, “Generation of broad-band chaos using blocking oscillator”, IEEE Transaction on Circuits and Systems-1, vol.48, No.6, 2001.

[13] YU. V. Andreyev, A. S. Dmitriev, E. V. Efremova, A. D. Khilinsky and L. V. Kuzmin, “Qualitative theory of dynamical systems, chaos and contemporary wireless communications” International Journal of Bifurcation and Chaos, Vol.15, No.11,(2005) 3639-3651.

[14] J. Guckenheimer and P. Holmes, Nonlinear Oscillations, Dynamical Systems, and Bifurcations of Vector Field. New York/ Springer-Verlag, 1983.

[15] J. C. Chedjou, K. Kyamakya, I. Moussa, H. –P. Kuchenbecker, W. Matis, “Behavior of a self-sustained Electromehanichal Transducer and Routes to Chaos”, Journal of vibrations and Acoustics, ASME Transactions, Vol. 128, pp 282-293, 2006.

[16] Thomas S. Parker and Leon O. Chua,”Chaos: A Tutorial for Engineers”, Proc. of the IEEE, Vol. 75, N° 8, August 1987.

[17] J. C. Chedjou, K. Kyamakya, Van Duc Nguyen, I. Moussa and J. Kengne” Performance evaluation of analog systems simulation methods for the analysis of nonlinear and chaotic modules in communications”, ISAST Transactions on Electronics and Signal processing, N°1, vol.2, 2008, pp71-82.

[18] K. H. PAE, S. J. HAHN, “Multistability and chaos in Plasma Diode”, Journal of Korean Society, Vol.42, February 2003, pp. S994-S999.

[19] David C. Hamill, “Learning about chaotic circuits with SPICE”, IEEE Transaction on Circuits and Systems, vol.36, No.1, February 1993.

[20] P. Antognettti, and G. Kuznetzov, “Semiconductor Device Modelling with SPICE”, 2nd edition(Mc Graw-Hill,NY), 1993.

[21] Chance M. Glenn, “Synthesis of a Fully-integrated Digital Signal Source for communication from Chaotic Dynamics-based Oscillations”, PhD thesis, Johns Hopkins University, January 2003.

[22] H. B. Fotsin, J. Daafouz, “Adaptive synchronization of uncertain chaotic Colpitts oscillators based on parameter identification”, Physics Letters A 339(2005) 304-315.